Journal of Fluorine Chemistry 130 (2009) 1069–1079

Contents lists available at ScienceDirect

Journal of Fluorine Chemistry

journal homepage: www.elsevier.com/locate/fluor

Review

Investigating acidity of metal fluoride surfaces by spectroscopic and chemical methods

John M. Winfield *

Department of Chemistry, University of Glasgow, Joseph Black Building, Glasgow G12 8QQ, Scotland, UK

ARTICLE INFO

Article history:
Received 5 May 2009
Received in revised form 14 July 2009
Accepted 21 July 2009
Available online 28 July 2009

Keywords:
Lewis acidity
Brønsted acidity
FTIR
[^{36}Cl] radiotracer
Catalysis
Aluminium(III) fluoride
Magnesium(II) fluoride
Hydroxy fluoride

ABSTRACT

Recent investigations into the surface acidity of some aluminium and magnesium fluorides and their derivatives are reviewed with emphases on relative acidities and accessibilities of surface sites. The high specific surface areas of the materials are ideal for their study, either by FTIR spectroscopy using various probe molecules that have different basicity and steric requirements or by carrying out probe reactions that are catalysed by acidic surfaces. Context for some of the recent work is provided by a summary of the commercial catalyst, fluorinated chromia and the related, fluorinated aluminas; a particular emphasis in these sections is their catalysis of reactions that involve carbon–halogen species. For the high surface area metal fluorides and their derivatives, room temperature dehydrochlorination of *tert*-butyl chloride, employing chlorine-36 labelling to detect surface adsorbed species, enables comparative studies of surface acidity to be undertaken.

Contents

1. Introduction . . . 1068
2. The experimental approach . . . 1069
3. Fluorinated chromia . . . 1070
4. Fluorinated alumina . . . 1071
5. Aluminium chlorofluoride (ACF) . . . 1071
6. Aluminium hydroxy fluorides having the hexagonal tungsten bronze (HTB) or pyrochlore structures . . . 1072
7. High surface area (HS) aluminium fluorides . . . 1074
8. High surface area (HS) magnesium fluorides . . . 1076
9. Conclusions . . . 1077
Acknowledgements . . . 1077
References . . . 1077

1. Introduction

Acidity is a concept that occurs often in the chemistry of molecular fluorides and acid–base reactions are widely studied. A rather different situation exists for the solid state however. In this state of matter the most important acid reagents or catalysts are binary oxides in which the other element is in a high or its highest oxidation state. Silicas, transitional aluminas and aluminosilicates are good examples. One reason why these materials are so important is that they have relatively large specific surface areas, typically 100 $m^2 g^{-1}$ or greater. Analogous binary fluorides, as conventionally prepared, are molecular and thus usually volatile, or exist as fluoride-bridged crystal types whose surface areas are small.

A potentially very important development, resulting from recent synthetic work, has been the design of new preparative routes, which yield binary fluorides and their derivatives that have large specific surface areas. Such materials can be amorphous to

* Tel.: +44 0 141 330 5134; fax: +44 0141 330 4888.
E-mail addresses: johnwin@chem.gla.ac.uk, mandj.winfield@ntlworld.com.

0022-1139/$ – see front matter © 2009 Elsevier B.V. All rights reserved.
doi:10.1016/j.jfluchem.2009.07.012

X-rays but are not always so [1–5]. One factor driving these developments in the synthesis and characterisation of new potential solid acids is the requirement to replace mineral acids by reagents and catalysts that will generate less waste in their reactions; the result is so-called 'Green Materials'.

Making comparisons among solid Lewis or Brønsted acids is more complicated than is the case when molecular acids are compared. The intrinsic strengths of the different types of surface acid site are important; however the densities of surface sites and the morphology of the surface are likely to be crucial in determining the effectiveness of a solid acid under reaction conditions. In this review two different approaches are described, both of which compare the surface properties of different metal fluorides: firstly, the use of FTIR spectroscopy with various basic probe compounds and, secondly, the use of acid catalysed dehydrochlorination of hydrochloroalkanes as a probe reaction for surface Lewis acidity with detection of adsorbed species being accomplished by means of [^{36}Cl] radio-labelling of the probe compound. These are the 'spectroscopic' and 'chemical' methods referred to in the title. Examples will be taken from recent collaborative work (acknowledged at the end of this review) on amorphous, high surface area binary fluorides and aluminium hydroxy fluorides, which have the hexagonal tungsten bronze or pyrochlore structures. Although reference is made to other catalytic processes that involve carbon–halogen compounds, notably in the sections dealing with fluorinated chromia and alumina, this review does not include detailed discussion of recently reviewed work in which high surface area, amorphous metal fluorides have been used as acidic heterogeneous catalysts [1]. A very recent example of catalysis by metal fluorides whose surfaces have been modified to exhibit Brønsted and Lewis acidity is, however, described at the end of the review.

2. The experimental approach

Compounds such as anhydrous hydrogen fluoride, aHF, boron trifluoride, often manipulated as $BF_3{\cdot}OEt_2$, and antimony pentafluoride oligomers, for example $(SbF_5)_3$, are three of the archetypal fluorine-containing molecular acids and, as such, are used very widely. Recent progress in approaches that use computational [6,7] and thermodynamic data [8] has enabled quantitative comparisons of molecular fluoride Lewis acidity, *via* F^- ion affinities, to be made; in principle it is now possible to select a molecular fluorine-containing Lewis acid of appropriate strength for any molecular reaction in which F-transfer is important.

In solid acids the intrinsic strength of a site, nominally at the surface of the solid, may be well modified by the accessibility of the site to a basic reactant or probe molecule. For example, in considering a solid acid catalyst as a replacement for HCl in the reaction between aniline and formaldehyde to give the polyurethane intermediate, diamino diphenyl methane (DADPM), attention must be paid to the accessibility of the acid sites to what are relatively bulky reactants. One solution is to use dealuminated zeolites, where access to acid sites is possible through the external surface [9]. In addition, changes to the form of the external structured surface affect the product isomer distribution.

In the context of the experimental work to be reviewed here, the intrinsic base strength and the steric requirement of any probe molecule used to investigate the acidity of a solid, will both determine the results obtained. The ability of a probe to access the pore structure (usually macropores or mesopores) must always be considered. Until relatively recently this situation was irrelevant to the study of the distribution of acid sites in solid metal fluorides, as these materials characteristically have small surface areas and little or no internal pore structure. As indicated by recent examples [1–5] this is no longer the case. The properties of such high surface area solids (sometimes referred to as nanostructured [1] or nanosized particulate solids [4]) are often radically different from those of conventionally prepared bulk fluorides. Illustrating what may happen is an atomistic molecular dynamics simulation of cubic nanoparticles of α-AlF_3 [10]. The properties of the surface sites of the nanoparticles are quite different, particularly the edge and corner sites. Strong Lewis acidity is to be expected, unlike in bulk α-AlF_3, and structural analogies can be made with the thermodynamically less stable forms, for example β-AlF_3. Both experimental approaches that underlie the data presented here benefit from the high surface areas encountered.

Fourier transform infra-red spectroscopy was one of the earliest techniques to be applied to investigate the surface acidity of metal fluorides. In two early studies of a range of aluminium fluorides and fluorinated oxides, pyridine (py) was used as the probe species [11,12] and in one case [11] these data were supplemented by using the CO molecule as an additional probe. The use of the sterically less demanding CO can lead to a greater discrimination among different types of Lewis site and this is illustrated in later sections of the review. The use of py has been ubiquitous in studies of acidic oxides and is an important feature of the studies involving fluorides reviewed here. Two vibrational modes of the adsorbed py are particularly important. The position of the ν_{8a} mode, 1590–1630 cm^{-1}, indicates the relative Lewis acid strength of the site under investigation, *higher* values being correlated with *increased* acid strength. The integrated intensity of the ν_{19b} mode (in the range 1440–1460 cm^{-1}) with knowledge of the appropriate molar absorptivity can be used to estimate the site surface density but care must be exercised as molar absorptivities are not transferable unless very similar materials are compared [13]. Brønsted acid sites of high strength can be detected using py bands at 1540–1560 and $>1630\ cm^{-1}$ but 2,6-dimethylpyridine, lutidine (lut) is a stronger base, although sterically more demanding than py. The very weak base CO can be used also to probe Brønsted acidity. Uses of all three probes are illustrated in later sections of this review. Detailed accounts of experimental procedures are widely available in the literature (e.g. [13,14]).

The use of reactions that involve carbon–halogen bonds to investigate and compare different metal fluoride and oxofluoride surfaces has developed from investigations of the behaviour of chlorofluorocarbons, hydrochlorofluorocarbons and hydrofluorocarbons at fluorinated oxide catalysts; some aspects of this work are discussed below in Sections 3 and 4 of this review. In Sections 5, 6, 7, and 8 the dehydrochlorination of *tert*-butyl chloride, which occurs at room temperature in the presence of fluorinated Lewis acid surfaces, is emphasised. Accounts of the various hydrochlorocarbon—solid Lewis acid catalyst systems that are precursors to the use of Bu^tCl as a Lewis acid probe and descriptions of experimental details of the radiotracer method used are available elsewhere [13,15,16].

Although in optimal cases anhydrous HCl, which results from the dehydrochlorination reaction, can be detected in the gas phase above the surface, the usefulness of the method developed in Glasgow is the result of using chlorine-36 labelled Bu^tCl. This long-lived, β^- emitting isotope [17] enables the presence of adsorbed species, i.e. $H^{36}Cl$, to be detected even when the extent of the reaction is insufficient for HCl to be detected spectroscopically in the gas phase. Complementary experiments which involve the direct exposure of $H^{36}Cl$ to the surface are usually carried out also, in order to provide confirmatory evidence for adsorption. In addition to the sensitivity of [^{36}Cl], the *in situ* nature of the experiments means that glove box and vacuum techniques can be used at all stages, thus minimising exposure of hydrolytically sensitive fluorides to trace moisture.

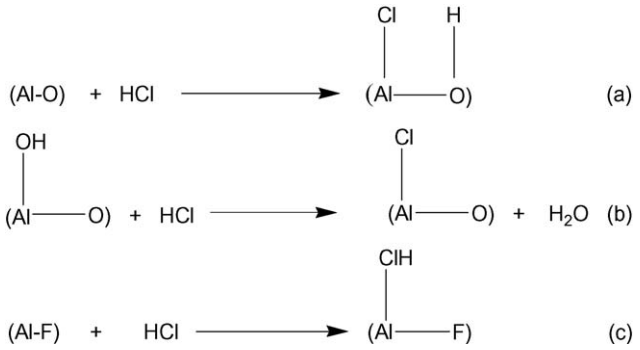

Fig. 1. Major (a) and minor (b) pathways proposed for the adsorption of anhydrous HCl at aluminas. From Ref. [18]. Reproduced by permission of Elsevier. In (c) an extension of the formulation is proposed to account for associative adsorption of HCl at an aluminium fluoride Lewis site.

There are two further aspects of the radiotracer labelled dehydrochlorination reaction approach that are worthy of mention. Firstly, due to the self-absorption properties [17] of β^- radiation (absorption by surrounding matter), the presence of [^{36}Cl] in the solid will not be detected by the Geiger Müller counters mounted directly above the surface [15], unless the isotope is located at the external gas–solid interface. This means that species adsorbed within the bulk, for example within the macroporous, mesoporous or even possibly the microporous structures that may be encountered, will not be detected unless and until they migrate to the exterior (gas–solid) surface. Potentially valuable information concerning the nature of the solid can therefore be inferred from the behaviour observed. A good example is the behaviour of H^{36}Cl towards aluminium hydroxy fluorides of the hexagonal tungsten bronze structural type, which is described in Section 6. Secondly, although the nature and geometry of the adsorbed species cannot be obtained directly from the radiotracer technique, there should be a profound difference between HCl chemically adsorbed at an oxide and its adsorbed state at a fluoride, in which 'oxidic islands' [11], originating from trace hydrolysis or from incomplete fluorination of an oxide surface, are absent. The possibilities are depicted in Fig. 1.

For oxides [18] and oxofluoride surfaces, dissociative adsorption is to be expected but, in the absence of trace surface hydrolysis of a metal fluoride, the most obvious possibility is that HCl will be associatively adsorbed, case (c) in Fig. 1. Since HCl is a very weak Lewis base, associative adsorption can be diagnostic for the presence of very strong Lewis acid sites. Although hydrogen bonding of HCl to surface F^- is also a possibility, it is considered to be less likely.

3. Fluorinated chromia

Chromia is probably the most widely used precursor for large scale catalytic fluorination processes, originally for C_2 chlorofluorocarbon production and more recently for hydrofluorocarbons such as 1,2,2,2-tetrafluoroethane (HFC-134a). The fluorinating agent is anhydrous HF and many years ago it was shown that fluoride-containing species, not all of which are catalytically active, are formed at the chromia surface during a catalytic fluorination reaction [19]. When fluorination of a C–Cl bond occurs, i.e. an F-for-Cl halogen exchange reaction, chloride is deposited at the fluorinated chromia surface and some of this can participate subsequently in a reverse Cl-for-F halogen exchange reaction [20]. The overall process of halogen exchange involving a C_2 chlorofluoro- or hydrofluorocarbon can be regarded therefore as two series of, non-concerted, F-for-Cl and Cl-for-F substitution processes each of which involves halogen transfer from surface to substrate and *vice versa*. Chloride can be deposited also on fluorinated chromias by means of anhydrous HCl [20,21]. This combination of fluorination and chlorination of the chromia

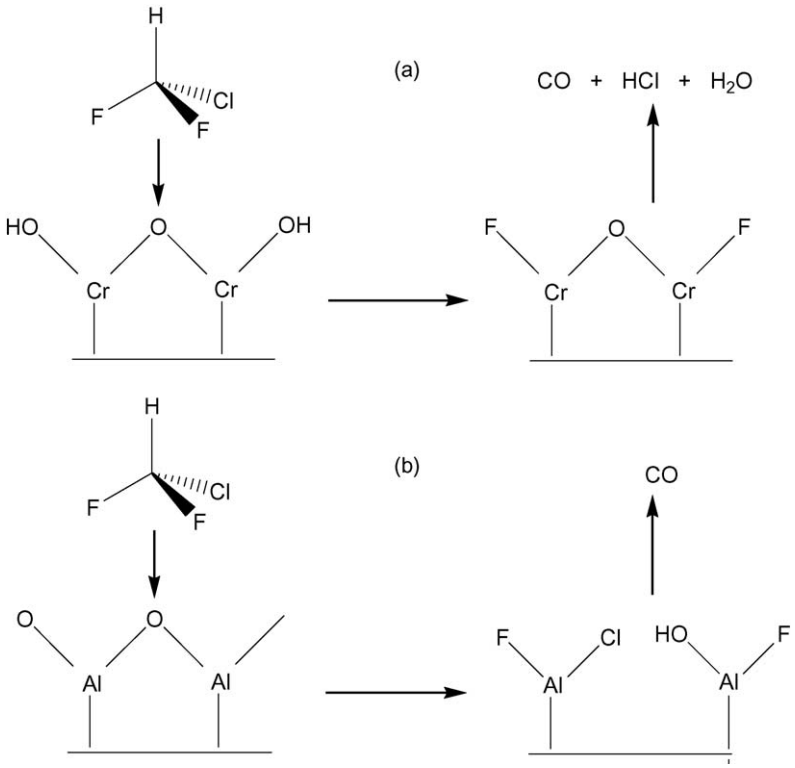

Fig. 2. Reactions that could occur between $CHClF_2$ (HCFC-22) and (a) chromia or (b) alumina, and which could result in the formation of halogenated surfaces. From Ref. [23]. Reproduced by permission of Elsevier.

surface is in part a reflection of the similar enthalpy changes occurring when Cr_2O_3 is fluorinated or chlorinated; this is in contrast to the analogous situation that involves alumina, where the thermodynamic preference is overwhelmingly for fluorination over chlorination [22,23].

A chromia surface may also be fluorinated by flow of C_1 CFCs or HCFCs, this being part of the activation process prior to catalytic reactions involving carbon–halogen species [22,23]. A proposed activation reaction involving $CHClF_2$ (HCFC-22) is depicted in Fig. 2(a).

The type of surface species formed from such reactions has received extensive study. There is no evidence for the formation of a simple chromium(III) oxofluoride (such as CrOF) in a fluorinated chromia synthesised from solid state reactions carried out under mild conditions; rather F replaces O in the Eskolaite, Cr_2O_3 lattice, leading to increased distortion as the F content increases. Gas phase fluorination of Cr_2O_3 leads to 'surface fluoride phases' [24]. Surface acidity, as determined by FTIR and py as the probe species, is significantly enhanced by fluorination; Lewis rather than Brønsted sites are characteristic. Activation of chromia by CCl_2F_2 flow results in mixed chromium oxide halide species on the surface rather than individual CrF_3 and $CrCl_3$ phases [25].

Investigations of the dynamic behaviour of HFCs influenced by the enhanced Lewis acidity of fluorinated chromias have been focussed on CH_2FCF_3 (HFC-134a), no doubt because of its commercial importance during the past 10 years. The halogen exchange model developed for C_2 CFCs appears, after the initial hydrofluorination of $CHCl{=}CCl_2$ to give CH_2ClCCl_2F, to be applicable here; unwanted dehydrofluorination processes that lead to toxic, olefinic side products can be inhibited by maintaining a good concentration of adsorbed HF at the surface [26,27]. The alternative pathway of dehydrochlorination or dehydrofluorination followed by hydrofluorination of the olefin formed can be promoted by using a chromia prefluorinated by an HFC. The isomerisation of CHF_2CHF_2 to CH_2FCF_3 occurs *via* this route [28,29].

4. Fluorinated alumina

In contrast to the chromia situation, discussed above, fluorination of Al_2O_3 is thermodynamically favoured over its chlorination [22,23]; this is reflected in differences in behaviour of C_2 CFCs at the two fluorinated surfaces [30]. Enhancement of surface acidity by flow of $CHClF_2$, Fig. 2(b), has been used commonly and is the precursor to the dismutation of $CHClF_2$ to give CHF_3 and $CHCl_3$, which is used as a demonstration of Lewis acidity [31]. It is proposed that uptake of F occurs initially at the oxide particle surface but that its incorporation into the subsurface layers is required to produce a catalyst with enhanced acid properties. From analyses of data from various surface science techniques, an F species characterised by single bond formation and an high effective charge is indicated [31]. Extensive fluorination of aluminas can often result in the formation of crystalline AlF_3 phases [30] but direct evidence for the formation of intermediate oxofluoride phase formation is rare. However, recently, convincing evidence has been presented [32] for the formation of, $Al_{2-x/3}O_{3-x}F_x$, $x = 0.23–0.13$, in the pyrohydrolysis of finely divided α-AlF_3, which was prepared using sol gel or solvothermal methods (akin to those used for compounds reported in Sections 6 and 7). Surface acidity studies of this material will be of great interest.

An alternative method of fluorinating a γ-alumina surface is by the hydrolysis of a volatile covalent fluoride at the surface, for example SF_4 whose reaction at the surface is very exothermic, in a closed system [33]. Both new Lewis and Brønsted sites are created, the latter possibly originating from adsorption of the hydrolysis product HF. This surface promotes reactions with CH_3CCl_3 and Bu^tCl; in both cases there is evidence for the formation of oligomeric organic species. The former dehydrochlorination reaction has been examined in some detail since the organic layers supported on fluorinated alumina are the basis for room temperature halogen exchange catalysts [34,35]. The catalytic activities of these surfaces are significantly greater than those of the conventional Lewis acid BF_3 supported on γ-alumina [36].

There are similarities between the dynamic behaviour of $C_2Cl_{6-n}F_n$ at fluorinated alumina *vis-á-vis* fluorinated chromia surfaces but in two respects their behaviour can be differentiated. Isomerism of CCl_2FCClF_2 to give the thermodynamically more stable isomer, CCl_3CF_3, is of greater importance at fluorinated alumina and the subsequent reactions that occur are better viewed as disproportionations rather than non-concerted halogen exchanges [30,37] Mechanistic studies of CCl_3CF_3 behaviour at the closely related, Lewis acid surface β-AlF_3, indicated that surface fluoride species are not involved in the rearrangements that occur [38].

5. Aluminium chlorofluoride (ACF)

Aluminium chlorofluoride (ACF) is the pivotal compound in this review since it can be regarded as the link between the fluorinated oxides described above and the nanoscopic materials to be described in Sections 6–8. This very strong, solid Lewis acid originates from DuPont and much of the exploration of its behaviour as a Lewis acid catalyst has been undertaken at DuPont Central Research and Development [39–44]. Its synthesis, from aluminium trichloride and various CFCs, HCFCs or hexafluoropropene, illustrates the thermodynamic preference for Al–F over Al–Cl bond formation, mentioned above [22,23]. However replacement of Al–Cl bonds is not complete, the stoichiometry of the very hygroscopic compound formed being $AlCl_xF_{3-x}$, $x = 0.05–0.3$. In many types of reaction, for example those which appear to involve polyfluoro-carbocation addition to tetrafluoroethene, the effectiveness of ACF rivals or, in some cases exceeds, that of the archetypal, binary fluoride molecular Lewis acid SbF_5. ACF has the advantage that it does not behave as an oxidising agent, unlike SbF_5; however it is deactivated rapidly by even trace water [42]. A characteristic reaction, that has been used to compare its acid properties with those of amorphous aluminium fluoride [1,2], is the facile isomerisation of 1,2-dibromohexafluoropropene to the 2,2′-isomer [43,45], a reaction that is reminiscent of CCl_2FCClF_2 isomerisation, which was described in the context of operational tests for Lewis acidity above.

ACF and its bromine analogue, ABF, are amorphous to X-rays; their structures have therefore been inferred from a variety of spectroscopic measurements which include IR, MAS NMR, XANES and EXFAS [46,47]. The structures proposed are based on three different types of six coordinated Al^{III} centres. Chlorine (or bromine) is distributed throughout, rather than being present as an AlX_3 phase and the X atoms are postulated to be bridged among three Al^{III} atoms. Specific surface areas are usually in the range 100–150 $m^2\ g^{-1}$, although a mesoporous structure appears to be absent [46]. FTIR spectroscopy with py as the surface probe demonstrates, as expected, the presence of significant Lewis acid sites; interestingly, it indicates also a small degree of Brønsted acidity, which is presumed to be the result of strongly bound surface H_2O converting Lewis to Brønsted sites [46]. This characteristic reaction of very strong, solid Lewis acids is illustrated further in Sections 7 and 8 below.

ACF provides a benchmark for the detection of surface Lewis acidity by means of room temperature dehydrochlorination of Bu^tCl with [^{36}Cl] labelling [15]. Surface [^{36}Cl] count data which

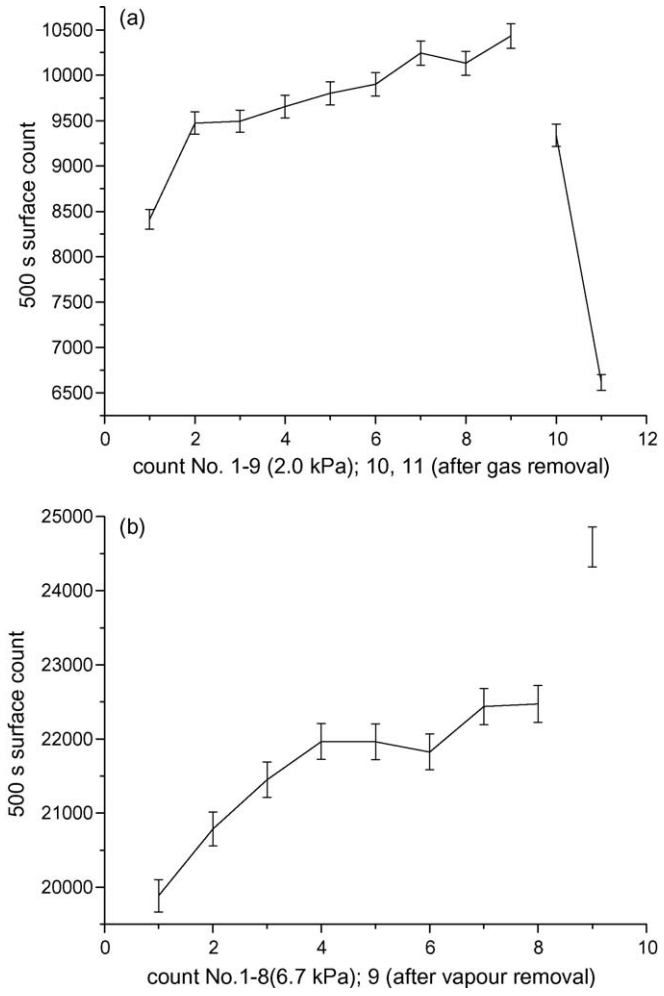

Fig. 3. [^{36}Cl] Surface count relationships from the successive additions of (a) H^{36}Cl and (b) [^{36}Cl]–Bu^{t}Cl to aluminium chlorofluoride (ACF). Line breaks correspond to the removal of the last aliquot of vapour. From Ref. [15]. Reproduced by permission of Elsevier.

result from exposures of series of aliquots of H^{36}Cl or [^{36}Cl]–Bu^{t}Cl to ACF surfaces are shown in Fig. 3(a) and (b) respectively.

The BET area of the sample used in these experiments was 100 m^2 g^{-1}, enabling achievement of good counting statistics, and the samples were handled throughout *in vacuo* or in a dry box. In each case there is a progressive build up of [^{36}Cl] activity as the number of exposures increases. Removal of the last aliquot of H^{36}Cl, after count 8 in Fig. 3(a), does not reduce the surface count to background; even after 24 h, count no. 11 in Fig. 3(a), the surface count is substantial. It appears therefore that exposure of H^{36}Cl to ACF results in the formation of both physically and chemically adsorbed species. Although some of the latter type may be H^{36}Cl, which is dissociatively adsorbed at a hydrated or hydroxylated site, cf. above and Fig. 1(a), it is considered that the data provide strong evidence for associatively adsorbed H^{36}Cl as in Fig. 1(c). The build up of [^{36}Cl] surface activity with successive exposures of [^{36}Cl]–Bu^{t}Cl, Fig. 3(b), is ascribed to adsorbed H^{36}Cl resulting from dehydrochlorination of the former. It is noteworthy that the final count in the series, count no. 9, recorded immediately after the removal of the last aliquot, shows an increase rather than the expected decrease. This can best be ascribed to an effect of [^{36}Cl] self-absorption, see Section 2 above and [17], and presumably involves migration of H^{36}Cl from a site in the bulk to the surface at which adsorption can be detected. Further examples of this phenomenon are given below.

6. Aluminium hydroxy fluorides having the hexagonal tungsten bronze (HTB) or pyrochlore structures

Aluminium hydroxy fluorides are potentially important solid acids, as in principle they may behave as Lewis acids *via* coordinatively unsaturated Al^{III} sites and as Brønsted acids *via* their hydroxyl groups. Accessibility is a possible constraint in both cases. There are two important structural types to consider, the hexagonal tungsten bronze (HTB) and the pyrochlore structures. In both cases hexagonal channels are a characteristic feature. The HTB structure is found for $AlF_{3-x}(OH)_x$ solids when x is small [48]; it is derived directly from the F-bridged HTB structure adopted by β-AlF_3 with hexagonal channels running along the c direction [49], the hydroxyl groups being isolated one from the other. The pyrochlore structure is found when the hydroxyl group content is greater; corner-sharing $Al(F,OH)_6$ octahedra are built up to form a three dimensional channel structure [50,51]. Because of the presence of −OH groups, the surface properties of both structural types may be complex. The use of more than one type of surface probe is advantageous when IR studies are contemplated. It should be remembered also that the –OH vibrational modes can give valuable information concerning the environment and relative Brønsted acid strength of particular types of –OH group present [52,53].

Transmission FTIR spectra obtained from py, 2,6-diMepy (lutidine, lut) and CO adsorbed at the surface of the HTB compound, $AlF_{2.6}(OH)_{0.4}$ are shown in Figs. 4–6 respectively [13]. The py and lut series of spectra (Figs. 4 and 5 respectively) represent adsorbed overlayers and the spectra that result from desorption at various temperatures. In contrast, the adsorbed layers of CO (Fig. 6) were obtained at 100 K and represent adsorption following successive doses of CO to the surface.

This compound originates from a microwave-assisted synthesis and is an assembly of nano-sized β-AlF_3 particles in which the HO-groups are the result of the reaction medium used, aqueous *iso*propanol/HF [4]. From a detailed analysis of the solid's powder XRD and MAS NMR spectra a structure has been proposed which comprises the structural motifs, 82% $[AlF_6]$ + $[AlF_5(OH)]$, 16% $[AlF_4(OH)_2]$ and 2% $[AlF_3(OH)_3]$ [4]. Its BET area is 82 m^2 g^{-1}, which is significantly greater than materials prepared by conventional means.

Spectral features due to the ν_{8a} and ν_{19b} are clearly recognisable ca. 1620 and 1454 cm^{-1} and indicate the presence of Lewis acid sites. However, there is no evidence for Brønsted acidity and the shift to lower energy observed for the surface ν(OH) mode is ascribed to hydrogen bonding with adsorbed py. Deconvolution of the ν_{8a} feature shows the presence of two components, a major component, 1620–1623 cm^{-1} and a minor at 1628 cm^{-1} (L_2 and L_1 in Fig. 4, inset B). At least two types of Lewis acid site are therefore present, with the stronger type being far less prevalent than the weaker. Spectra obtained from adsorption of the stronger base lutidine (lut), Fig. 5, provide evidence for both adsorbed and protonated lutidine in addition to physisorbed lutidine. There is a marked decrease in the intensity of the ν(OH) band at 3680 cm^{-1} (Fig. 5, inset), which is also consistent with Brønsted activity. Making comparisons with other cases of adsorbed lut suggests that a medium strong Brønsted acid is present, i.e. one insufficiently strong to protonate py but able to protonate the stronger base, lut [13].

The third basic probe used in this IR study was CO, which, because of its weakly basic character and the relatively large wavenumber range over which ν(CO) from adsorbed species is observed, is often very useful in discriminating among different types of surface acid site. As shown in Fig. 6, this is the situation for HTB-$AlF_{2.6}(OH)_{0.4}$. Feature E in the deconvoluted ν(CO) band envelope correlates with changes in the ν(OH) region (Fig. 6 inset)

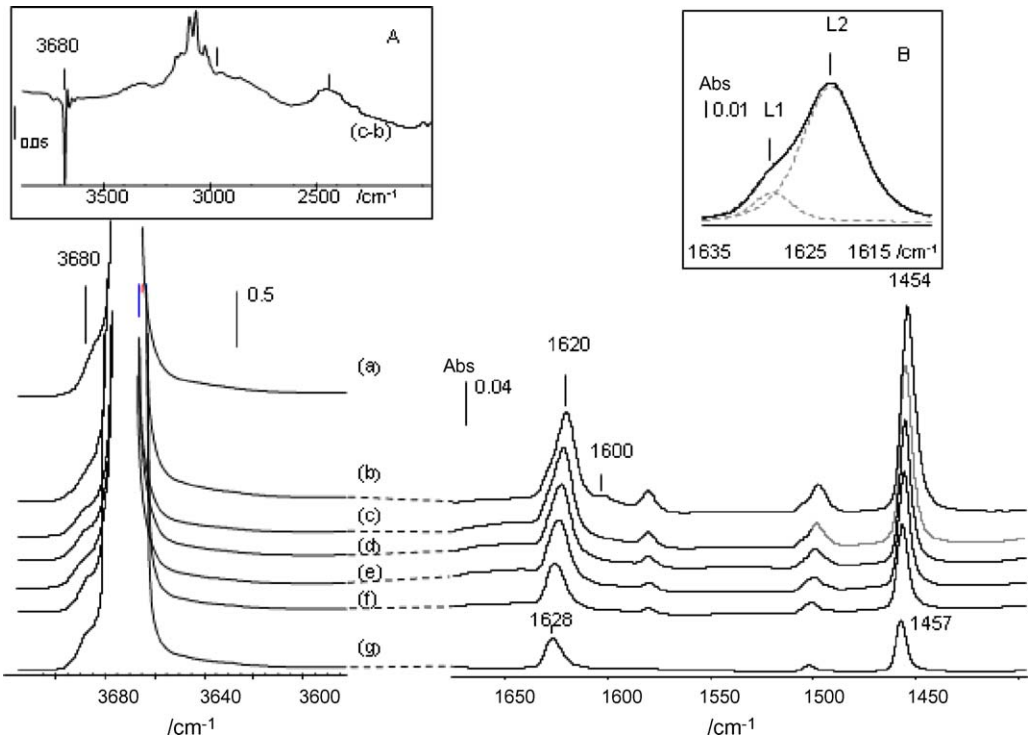

Fig. 4. IR spectra of β-$AlF_{2.6}(OH)_{0.4}$ after activation at 573 K before (a) and after introduction of an equilibrium pressure (133 Pa) of pyridine (b–g); (b) evacuation at room temperature under vacuum and thermodesorption at (c) 323, (d) 423, (e) 473, (f) 523 and (g) 573 K. Inset A: difference IR spectra after introduction of an equilibrium pressure (133 Pa) of pyridine followed by evacuation at r.t. Inset B: deconvolution (dotted lines) of the ν_{8a} vibrational mode (at room temperature). From Ref. [13]. Reproduced by permission of the PCCP Owner Societies.

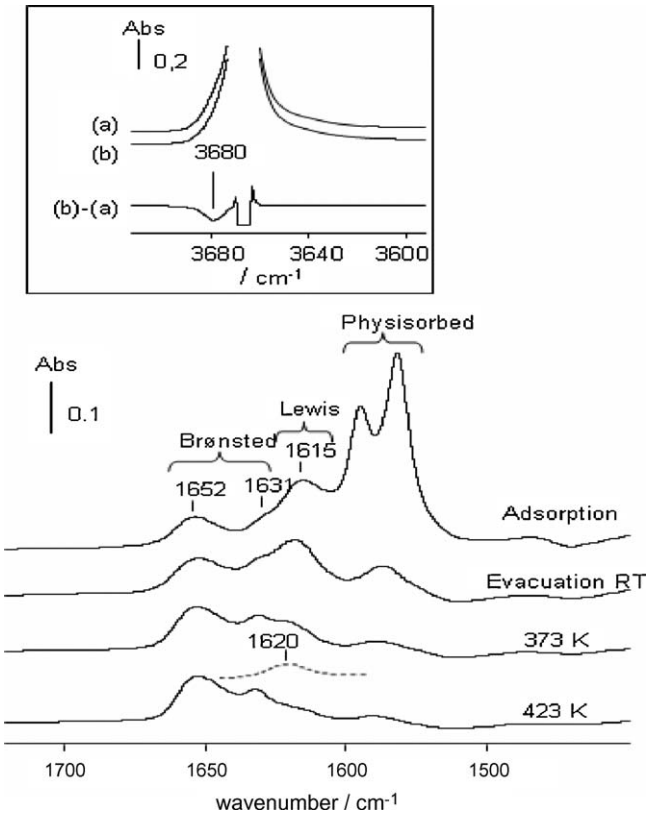

Fig. 5. Difference IR spectra of coordinated lutidine on β-$AlF_{2.6}(OH)_{0.4}$ after adsorption of 133 Pa at equilibrium pressure, followed by desorption under vacuum at room temperature (293 K), 373 and 423 K. The dotted curve is the difference curve between desorption obtained at 373 and 473 K. Inset: spectra in the ν(OH) region of the sample activated at 573 K (a) and after adsorption of lutidine (b). From Ref. [13]. Reproduced by permission of the PCCP Owner Societies.

and this feature is therefore assigned to a Brønsted acid site. The smaller width at half height of this feature compared with the remaining bands may mean that the –OH group has a symmetrical environment [13]. The remaining bands, A, B, C, D and F arise from Leis sites of differing relative strengths, the strongest site, A, being the least abundant. The assignments made are summarised in Table 1.

By means of co-adsorption experiments, in which py is first adsorbed then desorbed at a series of increasing temperatures with a CO pulse being introduced after each desorption step, it has proved possible to correlate sites detected using py with those detected by CO. Feature L_2 (from py spectra) correlated with sites C + D, while feature L_1 correlated with sites A + B [13].

The range of Lewis acid sites encountered in HTB-$AlF_{2.6}(OH)_{0.4}$ is a reflection of the integral role that hydroxyl groups play in its bulk structure, as opposed to being present as an impurity in β-AlF_3. Structural studies are consistent with the location of the HO– groups preferentially at bridging positions normal to the *c* axis and within the hexagonal channels [4] but it is reasonable to assume that the various F/OH coordination environments identified in the bulk will be reflected at the surface [13].

Surface hydroxyls and those located within the HTB channels provide sites for strong adsorption of $H^{36}Cl$ [13]. In this situation it is likely that –OH behaves as a Brønsted base towards the Brønsted acid HCl; alternatively, dissociative adsorption involving an hydroxyl group adjacent to a Lewis acid Al^{III} center or replacement of Al–OH by Al–Cl, cf. Fig. 1(a) and (b), are possibilities. However, room temperature dehydrochlorination of [^{36}Cl]–Bu^{t}Cl in the presence of solid $AlF_{2.6}(OH)_{0.4}$ is barely detectable. It can be observed and quantified however, by the addition of a small quantity of H_2O to give a solid of stoichiometry $AlF_{2.6}(OH)_{0.4}{\cdot}xH_2O$, x = 0.1–0.2 [13]. Possibly the presence of H_2O, located either in the hexagonal channels or coordinated to some surface Lewis sites promotes HCl adsorption as H_2O–HCl, similar to the situation found earlier for the interaction between $H^{36}Cl$ and β-AlF_3 [33].

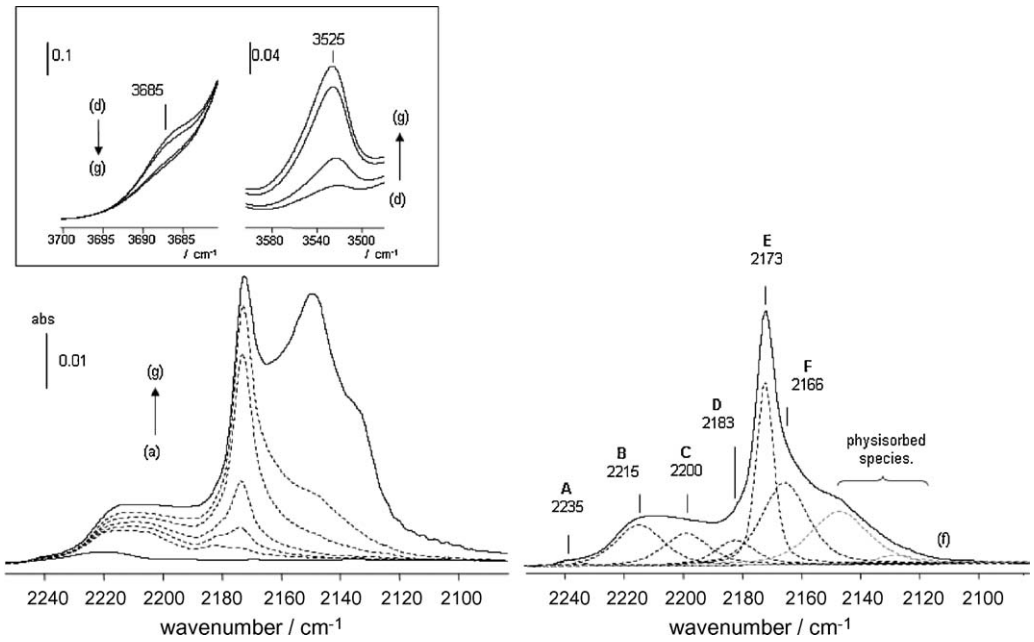

Fig. 6. Left: IR spectra recorded at 100 K after introduction of increasing CO doses at 100 K: 10 μmol g^{-1} (a), 44, 71, 88, 130, 300 μmol g^{-1} (b–f, respectively) then an equilibrium pressure (665 Pa) (g). Right: deconvolution of the ν(CO) band envelope on the spectrum (f). Inset: spectral region of the perturbed ν(OH) bands. From Ref. [13]. Reproduced by permission of the PCCP Owner Societies.

Table 1
IR ν_{max} data (cm^{-1}) for CO adsorbed at β-$AlF_{2.6}(OH)_{0.4}$[a].

β-$AlF_{2.6}(OH)_{0.4}$		Ranges for other CO_{ads} species[b]	Assignments[a]
ν(CO)	Assignment		
		2143	$CO_{(g)}$
		2140–2150	Physisorbed
2173	Medium Brønsted site	2150–2180	Brønsted site
2166	Very weak Lewis site	2160–2180	Weak Lewis site
2183	Weak Lewis site		
2220	Medium Lewis site	2180–2200	Medium Lewis site
2215–2220[c]	Strong Lewis site	2200–2220	Strong Lewis site
2235	Very strong Lewis site	>2220	Very strong Lewis site

[a] From Ref. [13].
[b] Cited in Ref. [59].
[c] Shifted to increased wavenumber with increasing coverage.

The properties of four HTB-structured aluminium fluorides, the two 'nanostructured' compounds discussed above and two conventionally prepared compounds are compared in Table 2 [13,33,53]. Compared with ACF the materials are less effective as Lewis acids, as judged by their behaviour with respect to dehydrochlorination of Bu^tCl, although they are effective Lewis acids with respect to py adsorption. The beneficial effect of an increase in specific surface area is apparent also from Table 2. Whereas evidence for the strongest Lewis sites at those materials having lower BET areas is masked at room temperature, it is recognizable, albeit by a shoulder on the main band, in $AlF_{2.6}(OH)_{0.4}$, suggesting that the proportion of strong Lewis sites in this material is greater. This is a particular case of what appears to be a general principle for Al^{III} fluorides that the number of Lewis sites is correlated to the specific surface area of the sample [54]. In turn this is a reflection of an increase in coordinatively unsaturated Al^{III} sites as particle size decreases [10].

In the nanostructured pyrochlore material, $AlF_{1.8}(OH)_{1.2}{\cdot}xH_2O$, which is prepared using a similar, microwave-assisted route to the HTB analogue, the determination of surface acidity can be made also using FTIR spectroscopy [5]. Water located within the channels is hydrogen bonded to F^- or –OH groups located nearby. The surface –OH groups result mainly in Brønsted acidity, while the Lewis acidity, probed using py and CD_3CN, is intermediate between that of γ-alumina (strong) and β-AlF_3 (very strong) [5]. As expected therefore, successive replacement of F by –OH or –O– results in decreasing Lewis acid strength for the surface sites.

7. High surface area (HS) aluminium fluorides

Development of a non-aqueous sol–gel technique for metal fluorides, with a subsequent vapour phase fluorination step, has led to a range of amorphous metal fluorides which have very large specific surface areas and mesoporous or sometimes microporous bulk structures [1]. Aluminium and magnesium fluorides and their derivatives have received particular attention; in this section the acidities of high surface area AlF_3, HS–AlF_3 [55–57], and its hydroxylated derivatives are discussed. Analogous magnesium fluorides are dealt with in Section 8.

There is abundant evidence that HS–AlF_3 behaves as a very strong Lewis acid, which in its catalytic behaviour, for example in the isomerisation of $CBrF_2CBrFCF_3$ to $CF_3CBr_2CF_3$, can be comparable to that of ACF. Here the use of basic probe species such as CO and room temperature dehydrochlorination of [^{36}Cl]–Bu^tCl at HS–AlF_3 surfaces are discussed.

Raman and IR spectroscopy, supported by detailed calculations provide an excellent way of differentiating among two crystalline phases, α and β, of AlF_3 and the amorphous HS–AlF_3 [58]; they are also helpful in providing context for the examination of surface acidity at HS–AlF_3. The relatively simple structural arrangement of AlF_6 octahedra in α-AlF_3 is probably the reason for the full vibrational analysis that is possible and for the excellent agreement between calculation and experiment. In the β phase (having the HTB structure [49]) two types of AlF_6 octahedra are present, which have different bond distances and bond angles. The corner-sharing pattern results in the presence of six- and three-membered rings and the resulting vibrational spectrum is very rich in detail. The study provides evidence for some disorder in the ring structure. Far less detail can be extracted from the spectra of HS–

Table 2
Comparisons among four aluminium fluoride derivatives, which have the HTB structure.

HTB surface	BET area ($m^2 g^{-1}$)	py ν_{8a} (cm^{-1})		Bu^tCl[a]	HCl[a]
β-AlF_3	26	1620	1627 (473 K)	Slow release of HCl (g)	Adsorption; desorption of H_2O–HCl
$AlF_{3-x}(OH)_3$ (× ca. 0.8)	ca. 30	1620	1627 (573 K)		
$AlF_{2.6}(OH)_{0.4}$	82	1620	1628 sh. (293 K)	Dehydrochlorination ability minimal	$H^{36}Cl$ strongly adsorbed
$AlF_{2.6}(OH)_{0.4}$, xH_2O (x = 0.1–0.2)	(82)			Moderate dehydrochlorination ability; promoted by H_2O?	adsorption, as H_2O–HCl?

[a] Behaviour at room temperature.

Table 3
IR ν_{max} data for CO adsorbed at β-AlF_3 and HS–AlF_3[a].

β-AlF_3 ν(CO)/cm^{-1} increasing coverage L to R, low to saturation					HS–AlF_3 ν(CO)/cm^{-1} increasing coverage L to R, low to saturation			Assignments
			2145				2150	Physisorbed
	2180	2170	2165		2180	2170	2170 sh	Medium-to-weak Lewis acid sites
2220	2220 sh							Strong Lewis acid sites
				2240–2235	2220		2220–2215	Very strong Lewis acid sites

[a] Data from Ref. [59].

AlF_3 but the very broad vibrational bands indicated a highly disordered structure in which resemblances to both α and β phases can be inferred [58].

In view of the disorder it is not surprising that the IR spectra of CO adsorbed at acid sites are complex. Interpretation of the spectra and those of CO adsorbed at β-AlF_3 is complicated by variations in ν(CO) IR bands with increasing CO coverage. However, ignoring effects on the spectra of possible CO–CO intermolecular interactions, it is possible to make proposals about Lewis acid site relative strengths and, to some extent, their relative abundances [59]. Some of the data obtained for HS–AlF_3 and β-AlF_3 are contained in Table 3.

The assignments of relative Lewis acid strength based on the positions of ν(CO), see also the data in Table 1, are to an extent subjective but are internally self-consistent. It is noteworthy that the highest value of ν(CO) found for HTB–$AlF_{2.6}(OH)_{0.4}$ (site A in Fig. 6) is rather similar to values for very strong Lewis sites at HS–AlF_3. The key feature in making comparisons however is not so much the band position but the relative proportion of the category of site being considered. The very high specific surface area of HS–AlF_3 as pointed out earlier [54] is a very important factor in determining its effectiveness as a Lewis acid. Similarly, in comparing the effectiveness of HS–AlF_3 with β-AlF_3 as Lewis acids, it is the relative proportions of strong and very strong sites which is the important comparator. On this basis HS–AlF_3 is expected to be the more effective [59] which is also consistent with the order of the two compounds' catalytic activities [1,55–57].

An identical conclusion is reached from consideration of room temperature dehydrochlorination of Bu^tCl in the presence of the two compounds. Exposure of HS–AlF_3 to Bu^tCl vapour at room temperature results in the immediate observation of HCl above the surface [16]; in contrast evolution of HCl when β-AlF_3 is exposed to Bu^tCl under identical conditions is a slow process [33]. The use of [^{36}Cl]–Bu^tCl enables interactions with the surface to be probed [16]; the behaviour observed in experiments that involve $H^{36}Cl$ or [^{36}Cl]–Bu^tCl, although not unlike that found for analogous experiments with ACF (Fig. 3), does depend to some extent on the history of the HS–AlF_3 sample used. [^{36}Cl] Surface count relationships that result from exposures of series of [^{36}Cl]–Bu^tCl aliquots to two different HS–AlF_3 samples are shown in Fig. 7.

The sample in (a) had been fluorinated in the final step of its preparation by flow of CCl_2F_2/N_2 at 423–573 K; its BET area was 180 $m^2 g^{-1}$. The sample used in (b) had been fluorinated at the final step using aHF/N_2 at 393 K; its BET area was 420 $m^2 g^{-1}$ [16]. The [^{36}Cl] specific count rate of the [^{36}Cl]–Bu^tCl used was identical in both experiments, therefore in (b), the higher surface counts and their greater precision can be assumed to be, at least partly, a reflection of the greater specific surface area. More important is the different behaviour observed for the adsorbed $H^{36}Cl$ after removal of the last aliquot of [^{36}Cl]–Bu^tCl. In Fig. 7(a) the final count (count no. 9) is greater than those determined previously, whereas in Fig. 7(b) the final two counts (nos. 9 and 10) are almost at the background level. It appears therefore that pre-treatment with CCl_2F_2/N_2 enables substantial chemisorption of $H^{36}Cl$ to occur and that dehydrochlorination occurs both at the exterior surface and within the bulk. This does not appear to be the case when fluorination is carried out using aHF/N_2.

Surface count data from three series of [^{36}Cl]–Bu^tCl exposures to each sample are summarised in Table 4. The first entries (run 1) in each case correspond to the data in Fig. 7(a) and (b).

Table 4
[^{36}Cl] Surface counts from multiple exposures of [^{36}Cl]–Bu^tCl to HS–AlF_3 samples[a] prepared either using CCl_2F_2/N_2 or aHF/N_2.

Fluorinating agent	Run no.	Mean surface count $(500\,s)^{-1}$ (no. of points)	Rel. error (%)	Retained surface count $(500\,s)^{-1}$	Rel. error (%)
CCl_2F_2	1	5531 (8)	4.7	6166	2.3
	2	9357 (8)	2.4	8796	1.7
	3	8904 (8)	2.2	8122	1.9
aHF	1	16303 (8)	2.4	1446 then 1645[b]	7.1, 6.0[b]
	2	9705 (9)	2.7	2011	5.2
	3	15197 (9)	4.2	1957 then 6780[b]	5.4, 2.1[b]

[a] BET areas were 180 (ex. CCl_2F_2) and 420 $m^2 g^{-1}$ (ex. aHF).
[b] Determined immediately on removal of volatile material, then 24 h later. Data are from Ref. [16] and are reproduced with permission from Elsevier.

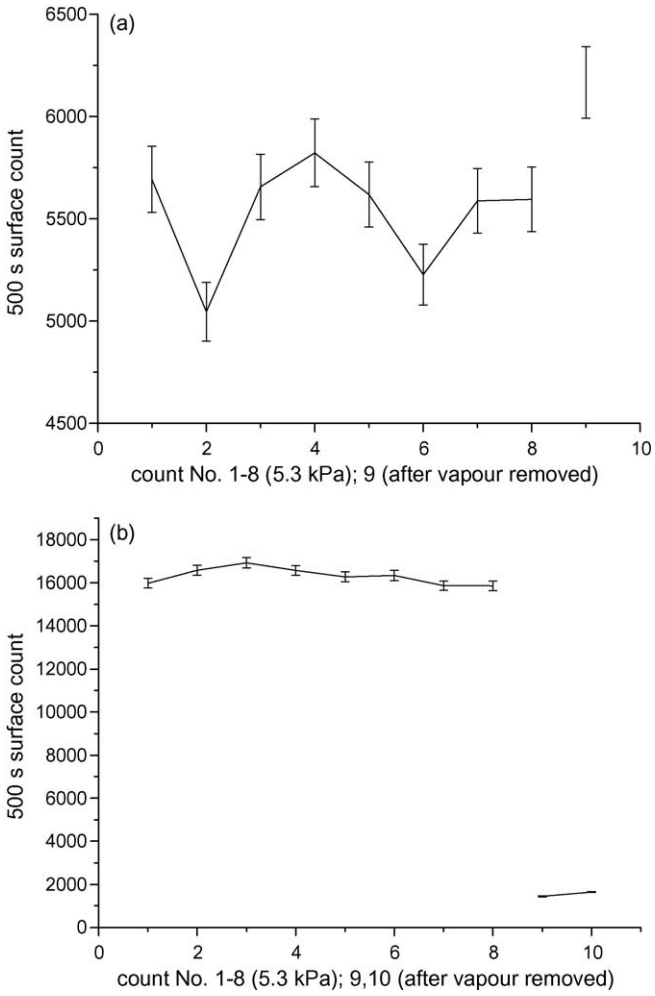

Fig. 7. Comparison of the behaviour of [^{36}Cl]–Bu^{t}Cl towards HS–AlF_3 samples whose precursors had been fluorinated with (a) CCl_2F_2/N_2 and (b) with HF/N_2; a set of sequential exposures is shown for each sample. Line breaks correspond to the removal of the last aliquot of vapour in a set; in (b) count 10 was recorded 1 d after count 9. Redrawn data from Ref. [16]. Reproduced by permission of Elsevier.

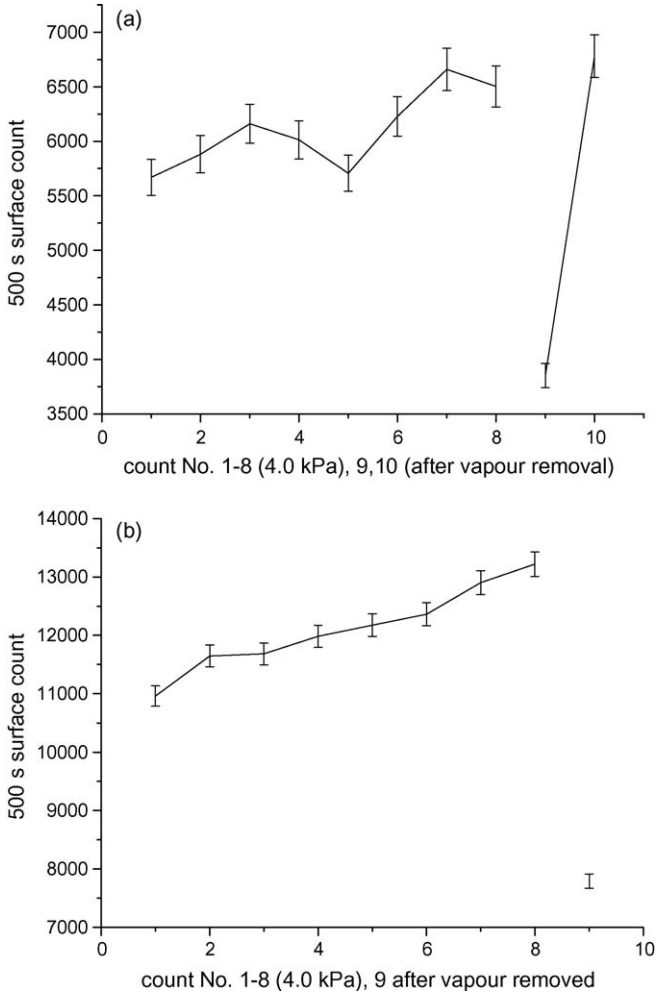

Fig. 8. Comparisons between [^{36}Cl] surface counts from [^{36}Cl]–Bu^{t}Cl aliquots in contact with (a) HS–MgF_2 and (b) 15 mol% HS–FeF_3 in HS–MgF_2. Line breaks correspond to the removal of the last aliquot of vapour. From Ref. [16]. Reproduced by permission of Elsevier.

Inspection of the data indicates that when CCl_2F_2 is used in the synthesis, there is a high degree of H^{36}Cl retention, of the order of 90% of the mean count. Since the data from runs 2 and 3 are effectively identical, it appears that the sites at which H^{36}Cl is adsorbed can become saturated. In contrast there is little evidence for the occurrence of strongly adsorbed H^{36}Cl when aHF is involved in the synthesis, until the end of run 3 in Table 4 at which point there appears to be migration of H^{36}Cl from the bulk to the exterior surface. The difference in behaviour can be rationalised by the assumption that aHF is adsorbed to some extent during its flow over the solid and that this has the effect of blocking subsequent H^{36}Cl adsorption, presumably in both cases at the strongest Lewis acid sites [16].

Blocking of strong surface Lewis sites by adsorption of H_2O has been observed using IR spectroscopy. For example a band at 3677 cm^{-1} is assigned to ν(OH); it is shifted substantially to lower wavenumber by subsequent adsorption of CO [59], in a manner similar to the behaviour of surface hydroxyl groups of HTB aluminium hydroxy fluorides [13] that were described in Section 6.

Deliberate introduction of H_2O in a controlled manner can lead therefore to Brønsted acidity [59] in HS–AlF_3 and the resulting 'tuned' Lewis plus Brønsted surfaces may have potential as catalysts. In a very recent example [60], a series of materials was prepared by introducing different quantities of water into the non-aqueous sol–gel synthesis. Examination of the surface acidity of the resulting HS–$AlF_{3-x}(OH)_x$ compounds using CO and lutidine (lut) as IR basic probes has led to the conclusion that this series has a relatively small proportion of strong Lewis sites coupled with higher proportions of Brønsted sites having weak or medium strength. We return to this point in the following section where analogous magnesium fluoride derivatives are discussed.

8. High surface area (HS) magnesium fluorides

When prepared by conventional means magnesium difluoride, which has the rutile structure, behaves as a basic fluoride; it has found some use as a support material in heterogeneous catalysis [61]. As prepared *via* the non-aqueous sol–gel route [2,3] however amorphous HS–MgF_2 exhibits behaviour characteristic of a Lewis acid of moderate strength. The behaviour of [^{36}Cl]–Bu^{t}Cl in the presence of HS–MgF_2, which is shown in Fig. 8(a), illustrates this very well [16].

Although there is no evidence for evolution of HCl to the gas phase above the surface, in contrast to the situation for HS–AlF_3, deposition of [^{36}Cl], presumed to be H^{36}Cl, at the surface is evident. As indicated in Fig. 8(a) a substantial proportion of this is strongly bound and some of it is located within the sample from which it migrates to the exterior surface over a period of time. The

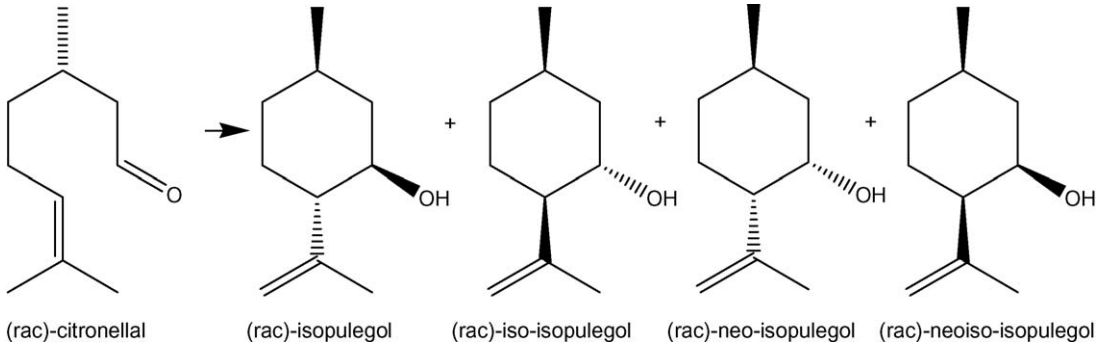

Fig. 9. The cyclisation of citronellal to isopulegols. From Ref. [63]. Reproduced by permission of the Royal Society of Chemistry.

behaviour of an HS–MgF_2 derivative, 15 mol% HS–FeF_3 in HS–MgF_2, is shown in Fig. 8(b). These two materials have almost identical BET areas and very similar pore structures [16], making it justifiable to compare behaviour of their [^{36}Cl] surface counts. The substantially greater surface counts in Fig. 8(b) compared with those in Fig. 8(a) suggest strongly that additional Lewis acid sites, presumably Fe^{III} based, are present in the Fe^{III}/Mg^{II} material. This is consistent with their behaviour with respect to NH_3 temperature programmed desorption experiments [16].

In a fashion similar to that described for HS–AlF_3 above [60], conducting the sol–gel synthesis in an organic/aqueous HF medium to which varying quantities of water are added, leads to $MgF_{2-x}(OH)_x$ materials which have Brønsted acidity in addition to functioning as Lewis acids of medium strength [62]. The aluminium and magnesium hydroxy fluorides that result from this type of synthesis are being evaluated as potential heterogeneous catalysts for fine chemicals syntheses in situations where combined Lewis and Brønsted acidity may be required. A recent example is shown in Fig. 9 and involves the cyclisation of citronellal to isopulegols.

This transformation is relevant to the large scale route to (−)-menthol, the key step being the isomerisation of (+)-citronellal to (−)-isopulegol with a high diastereoselectivity. The compound HS–AlF_3, although as described above is a strong Lewis acid, can exhibit some Brønsted acidity as a result of surface hydrolysis [59,60]. This compound and a range of $AlF_{3-x}(OH)_x$ and $MgF_{2-x}(OH)_x$ resulting from water introduced at the sol–gel step, are effective laboratory catalysts for batch conversion of citronellal to (±)-isopulegol (the major product) and (±)-neo-isopulegol [63]. The best activity and selectivity were found using catalysts that have very strong Lewis acid sites coupled with weak Brønsted acidity.

9. Conclusions

Recent advances in synthesis have enabled the development of new types of binary metal fluoride solid Lewis acids in which the nanostructured nature of the solids leads to surface acidity that is enhanced significantly over their conventionally prepared analogues. Brønsted acids are produced either from Lewis surface sites at which water has been coordinated or by the deliberate incorporation of hydroxyl groups during the synthesis. These materials can be related in their properties to traditional high surface area, partially fluorinated aluminas or chromia; a relationship exists also with the hydrolytically unstable amorphous solid aluminium chlorofluoride. Development of characteristic reaction methodology, in which the radio-isotope chlorine-36 can be used with advantage, enables comparisons among different acids to be made. FTIR spectroscopy, employing a range of basic molecules to probe the surface enables sites of differing relative strengths to be identified and their relative strengths compared.

Acknowledgements

Much of the work reviewed here was carried out through the FUNFLUOS network supported by the EU, contract no. NMP3-CJ-2004-5005575. The author is very grateful both to the EU and to members of the participating groups for many discussions and exchanges of data during the extended period in which collaborative work was carried out.

References

[1] St. Rüdiger, U. Groß, E. Kemnitz, J. Fluorine Chem. 128 (2007) 353–368; St. Rüdiger, E. Kemnitz, Dalton Trans. (2008) 1117–1127.
[2] St. Wuttke, G. Scholz, St. Rüdiger, E. Kemnitz, J. Mater. Chem. 17 (2007) 4980–4988.
[3] J. Krishna Murthy, U. Groβ, St. Rüdiger, E. Kemnitz, J.M. Winfield, J. Solid State Chem. 179 (2006) 739–746.
[4] D. Dambournet, A. Demourgues, C. Martineau, S. Pechev, J. Lhoste, J. Majimel, A. Vimont, J.-C. Lavalley, C. Legein, J.-Y. Buzaré, F. Fayon, A. Tressaud, Chem. Mater. 20 (2008) 1459–1469.
[5] D. Dambournet, A. Demourgues, C. Martineau, E. Durand, J. Majimel, A. Vimont, H. Leclerc, J.-C. Lavalley, M. Daturi, C. Legein, J.-Y. Buzaré, F. Fayon, A. Tressaud, J. Mater. Chem. 18 (2008) 2483–2493.
[6] K.O. Christe, D.A. Dixon, D. McLemore, W.W. Wilson, J.A. Sheehy, J.A. Boatz, J. Fluorine Chem. 101 (2000) 151–153; a set of revised pF data was presented by K. O. Christe, D. A. Dixon, Abs. ACS 19th Winter Fluorine Conference, Jan. 11–16, 2009, abs. no. 59 and will be published (K.O. Christe, personal communication).
[7] H.D.B. Jenkins, I. Krossing, J. Passmore, I. Raabe, J. Fluorine Chem. 125 (2004) 1585–1592.
[8] H.D.B. Jenkins, H.K. Roobottom, J. Passmore, Inorg. Chem. 42 (2003) 2886–2893.
[9] A. Corma, P. Botella, C. Mitchell, Chem. Commun. (2004) 2008–2010.
[10] S. Chaudhuri, P. Chupas, B.J. Morgan, P.A. Madden, C.P. Grey, Phys. Chem. Chem. Phys. 8 (2006) 5045–5055.
[11] C. Morterra, G. Cerrato, P. Cuzzato, A. Masiero, M. Padovan, J. Chem. Soc. Farad. Trans. 88 (1992) 2239–2350.
[12] A. Hess, E. Kemnitz, J. Catal. 149 (1994) 449–457.
[13] D. Dambournet, H. Leclerc, A. Vimont, J.-C. Lavalley, M. Nickkho-Amiry, M. Daturi, J.M. Winfield, Phys. Chem. Chem. Phys. 11 (2009) 1369–1379.
[14] E. Paven, J. Grimblot, J.-C. Lavalley, M. Daturi, F. Maugé, in: J.M. Chalmers, P.R. Griffith (Eds.), Handbook of Vibrational Spectroscopy, vol. 4, Wiley, New York, 2002.
[15] M. Nickkho-Amiry, J.M. Winfield, J. Fluorine Chem. 128 (2007) 344–352.
[16] M. Nickkho-Amiry, G. Eltanany, St. Wuttke, St. Rüdiger, E. Kemnitz, J.M. Winfield, J. Fluorine Chem. 129 (2008) 366–375.
[17] W.D. Ehmann, D.E. Vance, Radiochemistry and Nuclear Methods of Analysis, John Wiley and Sons, Inc., New York, 1991.
[18] A.R. McInroy, D.T. Lundie, J.M. Winfield, C.C. Dudman, P. Jones, S.F. Parker, D. Lennon, Catal. Today 114 (2006) 403–411.
[19] J. Kijowski, G. Webb, J.M. Winfield, Appl. Catal. 27 (1986) 181–193.
[20] L. Rowley, J. Thomson, G. Webb, J.M. Winfield, A. McCulloch, Appl. Catal. A 79 (1991) 89–103.
[21] H. Bozorgzadeh, E. Kemnitz, M. Nickkho-Amiry, T. Skapin, J.M. Winfield, J. Fluorine Chem. 121 (2003) 83–92.
[22] E. Kemnitz, D.-H. Menz, Prog. Solid State Chem. 26 (1998) 97–153.
[23] E. Kemnitz, J.M. Winfield, in: T. Nakajima, B. Žemva, A. Tressaud (Eds.), Advanced Inorganic Fluorides: Synthesis Characterization and Applications, Elsevier Science, S.A, Amsterdam, 2000 (Chapter 12).
[24] B. Adamczyk, O. Boese, N. Weiher, S.L.M. Schroeder, E. Kemnitz, J. Fluorine Chem. 101 (2000) 239–246.
[25] E. Ünveren, E. Kemnitz, U. Oran, W.E.S. Unger, J. Phys. Chem. B 108 (2004) 15454–15456.
[26] D.W. Bonniface, J.R. Fryer, P. Landon, J.D. Scott, W.D.S. Scott, M.J. Watson, G. Webb, J.M. Winfield, Green Chem. 1 (1999) 9–11.

[27] A.W. Baker, D. Bonniface, T.M. Klapötke, I. Nicol, J.D. Scott, W.D.S. Scott, R.R. Spence, M.J. Watson, G. Webb, J.M. Winfield, J. Fluorine Chem. 102 (2000) 279–284.
[28] E. Kemnitz, K.-U. Niedersen, J. Fluorine Chem. 79 (1996) 111–119.
[29] K.-U. Niedersen, K. Fiedler, E. Kemnitz, J. Fluorine Chem. 126 (2005) 1017–1027.
[30] H. Bozorgzadeh, E. Kemnitz, M. Nickkho-Amiry, T. Skapin, J.M. Winfield, J. Fluorine Chem. 110 (2001) 181–189.
[31] O. Boese, W.E.S. Unger, E. Kemnitz, S.L.M. Schoeder, Phys. Chem. Chem. Phys. 4 (2002) 2824–2832.
[32] M. Gaudon, J. Majimel, J.-M. Heintz, M. Feist, D. Dambournet, A. Tressaud, J. Fluorine Chem. 129 (2008) 1173–1179.
[33] C.H. Barclay, H. Bozorgzadeh, E. Kemnitz, M. Nickkho-Amiry, D.E.M. Ross, T. Skapin, J. Thomson, G. Webb, J.M. Winfield, J. Chem. Soc. Dalton Trans. (2002) 40–47.
[34] J. Thomson, G. Webb, J.M. Winfield, D. Bonniface, C. Shortman, N. Winterton, Appl. Catal. A 97 (1993) 67–76.
[35] A. Bendada, D.W. Bonniface, F. McMonagle, R. Marshall, C. Shortman, R.R. Spence, J. Thomson, G. Webb, J.M. Winfield, N. Winterton, Chem. Commun. (1996) 1947–1948.
[36] T.M. Klapötke, F. McMonagle, R.R. Spence, J.M. Winfield, J. Fluorine Chem. 127 (2006) 1446–1453.
[37] H. Bozorgzadeh, E. Kemnitz, M. Nickkho-Amiry, T. Skapin, J.M. Winfield, J. Fluorine Chem. 107 (2001) 45–52.
[38] H. Bozorgzadeh, E. Kemnitz, M. Nickkho-Amiry, T. Skapin, G.D. Tate, J.M. Winfield, J. Fluorine Chem. 112 (2001) 225–232.
[39] C.G. Krespan, A.C. Sievert, F.J. Weigert, PCT Int. Appl. WO. 91 05,753; Chem. Abs. 115 (1991) 70904q; C.G. Krespan, PCT Int. Appl. WO. 92 06,942; Chem. Abs. 117 (1992) 69439b.
[40] C.G. Krespan, D.A. Dixon, J. Fluorine Chem. 77 (1996) 117–126.
[41] V.A. Petrov, C.G. Krespan, B.E. Smart, J. Fluorine Chem. 77 (1996) 139–142.
[42] C.G. Krespan, V.A. Petrov, Chem. Rev. 96 (1996) 3269–3301.
[43] V.A. Petrov, C.G. Krespan, B.E. Smart, J. Fluorine Chem. 89 (1998) 125–130.
[44] V.A. Petrov, C.G. Krespan, J. Fluorine Chem. 102 (2000) 199–204.
[45] T. Krahl, R. Stösser, E. Kemnitz, G. Scholz, M. Feist, G. Silly, J.-Y. Buzaré, Inorg. Chem. 42 (2003) 6474–6483.
[46] T. Krahl, E. Kemnitz, J. Fluorine Chem. 127 (2006) 663–678.
[47] T. Krahl, E. Kemnitz, Angew. Chem. Int. Ed. 43 (2004) 6653–6656.
[48] A. Demourgues, L. Francke, E. Durand, A. Tressaud, J. Fluorine Chem. 114 (2002) 229–236.
[49] A. Le Bail, C. Jacoboni, M. Leblanc, R. De Pape, H. Duroy, J.L. Fourquet, J. Solid State Chem. 77 (1988) 96–101.
[50] J.L. Fourquet, M. Riviere, A. Le Bail, M. Nygrens, Eur. J. Solid State Inorg. Chem. 25 (1988) 535–540.
[51] R. König, G. Scholz, R. Bertram, E. Kemnitz, J. Fluorine Chem. 129 (2008) 598–606.
[52] L. Francke, E. Durand, A. Demourgues, A. Vimont, M. Daturi, A. Tressaud, J. Mater. Chem. 13 (2003) 2330–2340.
[53] A. Vimont, J.-C. Lavalley, L. Francke, A. Demourgues, A. Tressaud, M. Daturi, J. Phys. Chem. B 108 (2004) 3246–3255.
[54] D. Dambournet, G. Eltanamy, A. Vimont, J.-C. Lavalley, J.-M. Goupil, A. Demourgues, E. Durand, J. Majimel, St. Rüdiger, E. Kemnitz, J.M. Winfield, A. Tressaud, Chem. Eur. J. 14 (2008) 6205–6212.
[55] E. Kemnitz, U. Groβ, St. Rüdiger, S. Chandra Shekar, Angew. Chem. Int. Ed. 42 (2003) 4251–4254.
[56] K. St. Ruediger, U. Groβ, M. Feist, H.A. Prescott, S. Chandra Shekar, S.I. Troyanov, E. Kemnitz, J. Mater. Chem. 15 (2005) 588–597.
[57] St. Rüdiger, G. Eltanany, U. Groβ, E. Kemnitz, J. Sol–Gel Sci. Technol. 41 (2007) 299–311.
[58] U. Gross, St. Rüdiger, E. Kemnitz, K.-W. Brzezinka, S. Mukopadhyay, C. Bailey, A. Wander, N. Harrison, J. Phys. Chem. A 111 (2007) 5813–5819.
[59] T. Krahl, A. Vimont, G. Eltanany, M. Daturi, E. Kemnitz, J. Phys. Chem. C 111 (2007) 18317–18325.
[60] S.M. Coman, S. Wuttke, A. Vimont, M. Daturi, E. Kemnitz, Adv. Synth. Catal. 350 (2008) 2517–2524.
[61] M. Wojciechowska, M. Zieliński, M. Pietrowski, J. Fluorine Chem. 120 (2003) 1–11.
[62] St. Wuttke, S.M. Coman, G. Scholz, H. Kirmse, A. Vimont, M. Daturi, S.L.M. Schroeder, E. Kemnitz, Chem. Eur. J. 14 (2008) 11488–11499.
[63] S.M. Coman, P. Patil, St. Wuttke, E. Kemnitz, Chem. Commun. (2009) 460–462.